

Searching for the Next Yukawa Phase of QCD*

Miklos GYULASSY

*Physics Department, Columbia University,
New York, NY 10027*

Abstract

QCD predicts that the interactions between quarks and gluons change from a confining to a screened Yukawa form above a critical temperature $T_c \sim 150$ MeV. In this talk, I review some of the key observables in heavy ion reactions which are being used to search for this new partonic Yukawa phase at SPS and RHIC. These include collective observables such as dE_\perp/dyd^2p_\perp , meson interferometry, jet quenching, and J/ψ suppression.

* Talk to be published in the Proc. of 14th Nishinomiya-Yukawa Memorial Symposium Nov. 1999, Japan; updated with a critique of the CERN press release Feb. 8, 2000

§1. The Ubiquitous Yukawa

In 1935 H. Yukawa¹⁾ proposed a theory of nuclear forces based on the exchange of a massive boson

$$V_Y(r, m) = \alpha_{eff} \frac{e^{-mr}}{r} \quad (1.1)$$

He estimated that $m \sim 100$ MeV to account for the short range ~ 2 fm, and in 1947 Powell discovered the pion and confirmed this theory. An important theoretical precursor was the Klein-Gordon equation²⁾, whose static Green's function is (1.1). Elaboration of Yukawa's meson theory since then (including spin, orbit, isospin vertex factors) forms the basis for the present effective theory of nuclear forces^{3), 4)}.

In the unrelated field of electrolytes, Debye and Hückle had also come across the Yukawa potential in another context. It emerged from solving the Poisson equation in a conducting medium⁵⁾. Assuming that local charge density fluctuations occur with a Boltzmann probability, $\exp(-q\phi(x)/T)$, the polarizability of the medium in the presence of an external charge density, leads to a non-linear self consistent equation

$$\nabla\phi(x) = -4\pi(\rho_{ex}(x) + \sum_q qn_q e^{-q\phi(x)/T}) \ . \quad (1.2)$$

In the linearized approximation, the solution for a point charge is again eq. (1.1), but in this case the effective mass is the Debye electric screening mass

$$\mu^2 = 4\pi \sum_q q^2 |n_q| / T \ . \quad (1.3)$$

A dense conductive medium therefore transforms Coulomb into Yukawa.

In nuclear theory, the Yukawa meson mass results from the finite gap of the elementary excitations (pions, ...) of the physical QCD vacuum. By analogy, it should be possible to modify the nuclear Yukawa potential by increasing the nuclear density or temperature. In this talk I discuss current efforts to try to manipulate nuclear matter in the laboratory to force a breakdown of Yukawa's hadronic theory. As we will see, however, it seems difficult to escape from Yukawa. In the new deconfined, chirally symmetric phase of QCD at high temperatures, the Debye-Hückle mechanism takes over and the Yukawa potential between nucleons mutates into a color-electric screened Yukawa potential between partons of a quark-gluon plasma.

In QCD, the color potential between partons is approximately Coulombic at small distances due to the asymptotic freedom property of non-Abelian gauge theories. However, below a critical temperature, $T_c \sim 150$ MeV, the confinement property of the *nonperturbative* QCD vacuum allows only composite color singlet objects (hadrons) to "roam freely" in

the laboratory. The effective potential between the colored partons has a long range linear confining term κr to prevent them to roaming more than 1 fm away from any color neutral blob (hadrons). The restraining force or "string" tension, $\kappa \sim 1$ GeV/fm, is huge. In this confining phase of QCD, the heavy $q\bar{q}$ potential is well parameterized by the Lüscher form⁶⁾

$$V_L(r, 0) = -\frac{\alpha_L}{r} + \kappa r \quad , \quad (1.4)$$

(as long as dynamical quark pair production is ignored). The Coulombic part, with strength $\alpha_L = \pi/12$, arises from the zero point quantum fluctuations of the string (see p. 803 of Ref⁷⁾ for an intuitive derivation). This confining potential between heavy quarks has been directly observed numerically using lattice QCD techniques⁸⁾. As the temperature increases, but remains below the deconfinement transition, $T < T_c$, the enhanced fluctuations due to thermal agitation of the string modifies the effective potential into the approximate Gao form⁹⁾

$$V_G(r, T) = -\alpha_L \left[1 - \frac{2}{\pi} \tan^{-1}(2rT) \right] \frac{1}{r} + \left[\kappa - \frac{\pi}{3} T^2 \left(1 - \frac{2}{\pi} \tan^{-1}\left(\frac{1}{2rT}\right) \right) \right] r + \frac{T}{2} \ln(1 + (2rT)^2) \quad (1.5)$$

The decrease of the effective string tension, $\kappa(T)$, predicted above has been also observed in lattice QCD calculations¹⁰⁾ as shown in Fig.(1). However, the "measured" string tension is found to decrease faster than predicted in eq.(1.5) near the critical temperature. Note that in Fig.(1) $\beta = 2N_c/g^2 = \beta_c + \frac{12}{11N_c - 2N_f} \log(T/T_c)$, i.e., $T \approx T_c \exp(11/6(\beta - \beta_c))$ with $\beta_c = 4.0729$ for this lattice calculation.

For temperatures above T_c , we see from Fig.1 that a new Yukawa phase of QCD is predicted, and that the heavy quark potential mutates into a short range generalized Yukawa form, which on the lattice is measured in the form

$$V_L(r, T, d) = -\frac{\alpha(T)T}{(rT)^{d_L/2}} e^{-\mu_L(T)r/2} \quad . \quad (1.6)$$

Note that $d_L = 2, \mu_L(T) = 2m_E(T)$ correspond to a pure Yukawa interaction in terms of the lattice QCD fit parameters (d_L, μ_L) . The perturbative thermal QCD chromo-electric Debye mass $m_E = \mu(T)/2$ is¹²⁾

$$m_E(T) = g(T)T \left(\frac{N_c}{3} + \frac{N_f}{6} \right)^{1/2} \quad (1.7)$$

for N_c colors and N_f flavors. For $N_c = 2, N_f = 0$ in Fig. (1), we expect $\mu_L(T) = 2m_E = 1.6g(T)T$ as shown by the solid line in Fig.(2). The fits to the lattice QCD measurements Fig.(1 b) from¹⁰⁾ show that for $T > 2T_c$ $\mu_L \approx 2.5T$ is not far from the pQCD estimate. However, the exponent $d_L \approx 1.5$ is significantly below the value 2 expected from pQCD.

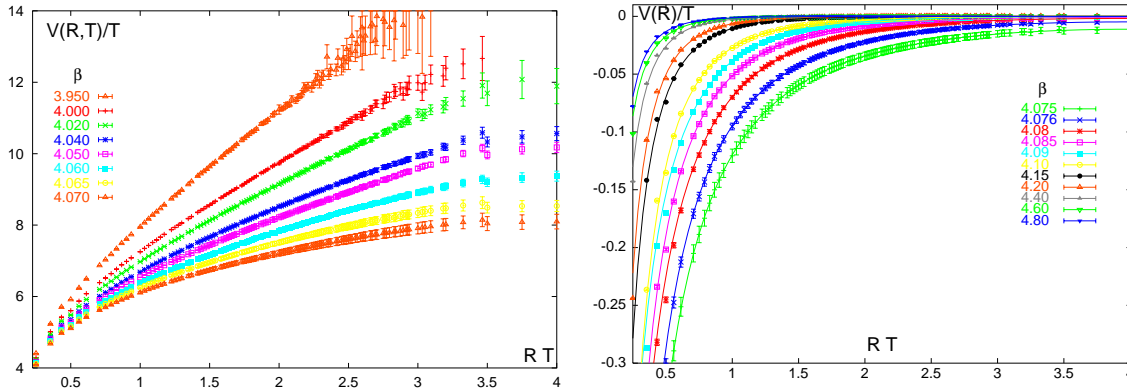


Fig. 1. (a) The heavy quark potential in the confined phase of SU(2) quenched QCD (left side) compared to that in the deconfined Yukawa phase above T_c (right side). Results are for a $32^3 \times 4$ lattice from Karsch et al¹⁰⁾. Eq.(1.5) fits the confined lattice "data" well, but the QCD string tension decreases more rapidly near T_c . For $T > T_c$ the potential is screened by the deconfined gluons (in this quenched calculation) and acquires the generalized Yukawa form (1.6). Here $T \approx T_c \exp(11/6(\beta - \beta_c))$ with $\beta_c = 4.0729$ and the lattice spacing is $a = 1/4T$.

An even more striking nonperturbative deviation is seen near T_c , at which point $d < 1$ and $\mu \sim T/2$. This suggests a rather long range interaction that may be the precursor of the confinement transition. This strong deviation from the perturbative QCD near T_c was also

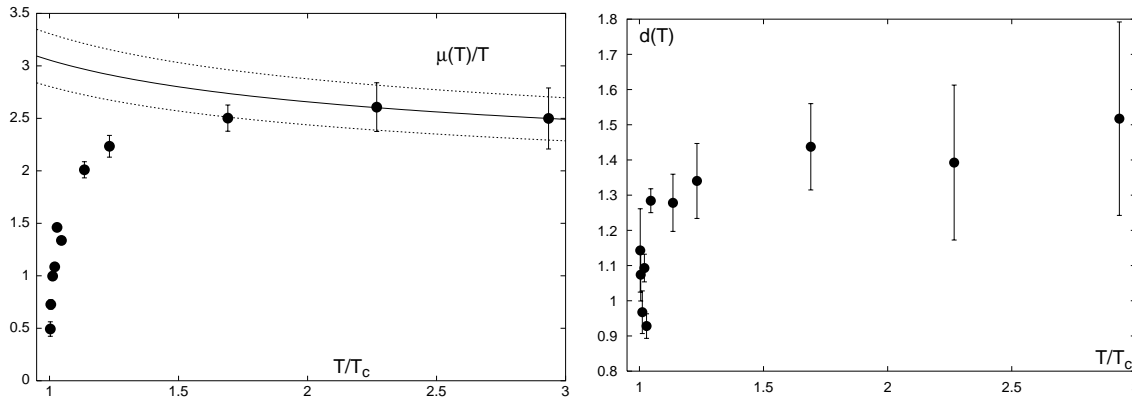


Fig. 2. The chromo-electric Debye screening mass, $\mu(T) = 2m_E(T)$ and the effective exponent, $d(T)$, of the effective Yukawa potential in the deconfined phase versus T/T_c is shown from Karsch et al¹⁰⁾ for SU(2) quenched QCD. The lines show expected dependence based on thermal pQCD. Note that near T_c , the range $2/\mu$ is much larger than predicted by pQCD and that $d \approx 1$ implies an especially long range interaction there.

reported previously in ref.¹¹⁾, where in addition it was found that the effective coupling is rather small $\alpha \sim 0.15$ above T_c . It is important to keep in mind that the above numerical experiments do not include dynamical quarks and are limited to SU(2). Nevertheless, they provide strong evidence that QCD predicts a qualitatively new (nonperturbative) partonic

Yukawa phase of matter that should exist at an energy density only an order of magnitude above that in ground state nuclei ($\epsilon > 2 \text{ GeV}/\text{fm}^3$).

The thermodynamic properties of the deconfined QCD phase are shown in Fig.3 from ref. ¹³⁾ for 2 flavor $12^3 \times 6$ IQCD. A present limitation of all lattice results so far is that the pion is still too massive to make contact with the “known” thermodynamic properties of ordinary hadronic/nuclear matter below T_c . Recent advances in implementing Domain Wall Fermions on the lattice and the availability of new TeraFlop scale computers at Columbia and the Riken Brookhaven Research Center ¹⁴⁾ and the CP-PACS project in Tsukuba ¹⁵⁾, should enable much more precise calculations of the quark-gluon plasma equation of state in the near future. Two striking features of Fig.(3) suggest two key observable signatures of this phase

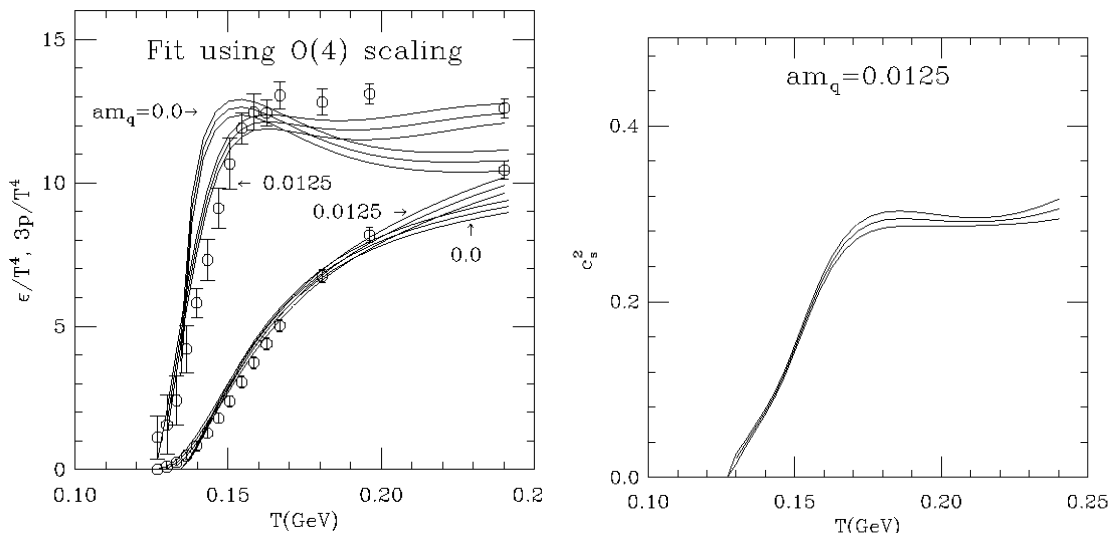


Fig. 3. Thermodynamic energy density (ϵ/T^4 top curves left), pressure ($3p/T^4$ lower curves left) and speed of sound squared (right) from lattice QCD (2 flavor $12^3 \times 6$) from the MILC collab ¹³⁾. The curves are zero quark mass extrapolations. Note the rapid reduction of the pressure and speed of sound as T_c is approached from above.

transition in nuclear collisions. First, the entropy density $\sigma(T) = (\epsilon + p)/T$ increase very rapidly with T in a narrow interval $\Delta T/T_c < 0.1$. Second, the plasma becomes extremely soft $p/\epsilon \ll 1$ and $c_s^2 \ll 1$ near T_c . As we review below, the first feature can lead to time delay (the QGP stall) measurable via hadronic interferometry. The second feature can lead to interesting non-linear collective flow observables in nuclear collisions. The experimental verification of these fundamental predictions of QCD is the primary motivation for the heavy ion experimental program at Brookhaven and CERN. In the following sections, I review first how deep into the QGP phase RHIC may be able to reach, and then discuss several signatures used to test the QCD predictions in such experiments.

§2. Initial conditions in A+A

In order to see the partonic Yukawa phase, we must first create an extended blob of matter at 100 times the density of nuclear matter. Head on collisions of heavy ions are used for that. There are many ways to describe how this dense matter is formed. One intuitive picture is given in terms of the McLerran-Venugopalan model¹⁶⁾. For highly boosted nuclei with $E_{cm} \sim 100m_N$, time dilation effectively freezes out the quantum chromo fluctuations inside the nuclei while the two pass through each other. Heavy Au beams can then be regarded as well collimated, ultra dense beams of partons. This (chromo Weizsacker-Williams) gluon cloud contains a very large number, $G_A(x, p_0^2) \sim A/x^{1+\delta}$, of almost on-shell collinear gluons with longitudinal momentum fraction $x = p_0/E_{cm} \ll 1$. As the clouds pass through each other, partons scatter via chromo Rutherford and decohere into a mostly gluon plasma on a fast time scale $1/p_\perp \ll 1$ fm/c. The number of gluons pairs (mini-jets) extracted from the nuclei by this mechanism at rapidities y_i and transverse momentum $\pm k_\perp$ can be calculated in pQCD as follows^{17), 18), 19), 20)}

$$\frac{dN_{AB \rightarrow ggX}}{dy_1 dy_2 dk_\perp^2} = K x_1 G_A(x_1, k_\perp^2) x_2 G_B(x_2, k_\perp^2) \frac{d\sigma_{gg \rightarrow gg}}{dk_\perp^2} T_{AB}(\vec{b}) \quad , \quad (2.1)$$

where $x_1 = x_\perp(\exp(y_1) + \exp(y_2))$ and $x_2 = x_\perp(\exp(-y_1) + \exp(-y_2))$, with $x_\perp = k_\perp/\sqrt{s}$, and where the pQCD $gg \rightarrow gg$ cross section for scattering with $t = -k_\perp^2(1 + \exp(y_2 - y_1))$ and $y_2 - y_1 = y$ is given by

$$\frac{d\sigma^{gg}}{dt} = \frac{9}{8} \frac{4\pi\alpha^2}{k_\perp^4} \frac{(1 + e^y + e^{-y})^3}{(e^{y/2} + e^{-y/2})^6} \quad . \quad (2.2)$$

The nuclear baryon number, A , only plays here the role of increasing the density of partons and providing the geometrical amplification, $T_{AB}(\vec{b}) \lesssim 30/\text{mb}$, for the number of binary nucleon-nucleon collisions that occur per unit area. A factor $K \sim 2$ simulates next to leading order corrections.

For symmetric systems, $A + A$, with $G_A \approx AG$. the inclusive gluon jet production cross section is obtained by integrating over y_2 with $y_1 = y$ and k_\perp fixed. To about 50% accuracy, the single inclusive gluon rapidity density in central collisions can be estimated by the following simple pocket formula²⁰⁾

$$\frac{dN}{dydt} \approx \frac{A^2}{\pi R^2} 2N_g(x_\perp, t) x_\perp G(x_\perp, t) \left(\frac{d\sigma_{gg}^{el}}{dt} \right)_R \propto A^{4/3} \quad (2.3)$$

where $N_g(x_\perp, t) = \int_{x_\perp}^1 dx G(x, t)$ is the total number of ‘‘hard’’ gluons coming down the beam pipe in an nuclear area πR^2 that can knock out unsuspecting gluons from the other nucleus.

This copious mini-jet mechanism is believed to be the dominant source of the gluon plasma that will be created when RHIC (finally) begins operation.

Recent upper bound estimates of the total gluon rapidity density as a function of the CM energy from ¹⁷⁾ are shown in Fig.(4). The differential yields are integrated down to a

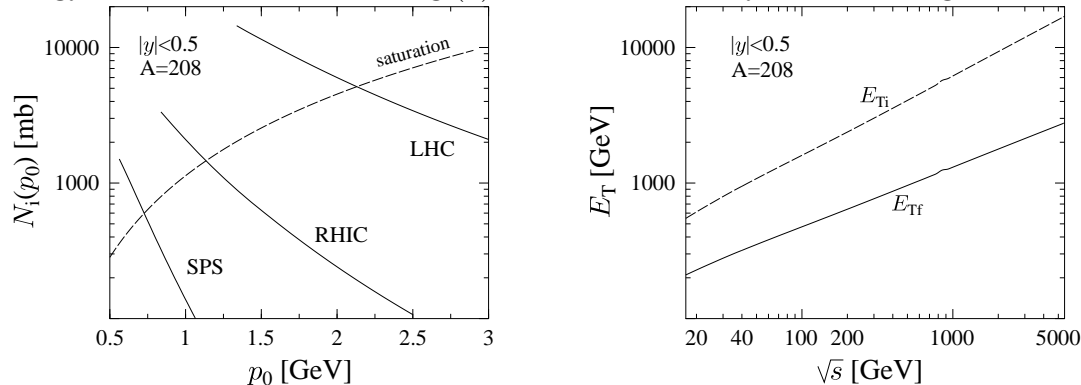


Fig. 4. Expected copious mini-jet production in A+A collisions from ref. ¹⁷⁾. The dashed curves in both figures correspond to an estimated maximum number (saturation) at which the nuclear area is filled with closed packed mini jet gluons ($N(p_0) = p_0^2 R^2$). (N_i is dimensionless, [mb] is a typo in fig.). The magnitude of possible hydrodynamic transverse energy loss due to longitudinal work in an ideal $p = \epsilon/3$ quark gluon plasma is shown by E_{Tf} .

transverse momentum scale $p_0 \sim 1 - 2$ GeV. This scale separates the “soft” nonperturbative beam jet fragmentation domain from the calculable perturbative one above. The curve marked saturation ¹⁹⁾ is an upper bound marking the point where the transverse gluon density of mini-jets becomes so high that the newly liberated gluons completely fill the nuclear area, i.e., $dN/dy \approx p_0^2 R^2$. At that point, higher order gluon absorption may limit the further increase of the gluon number. At RHIC energies these estimates yield up to 1500 gluons per unit rapidity. My more conservative estimates together with X.N. Wang ^{21), 22)} gives 500 gluons per unit rapidity when initial and final state radiation is also taken into account. This is obtained with a fixed $p_0 = 2$ GeV, that was found to be consistent with all available $p\bar{p}$ and low energy AA data using the HIJING mini-jet event.

The energy dependence of the final charged particle rapidity density from HIJING, including soft beam jet fragmentation, is shown in Fig.(5). Approximately one half of the height “Mt. RHIC” comes from soft beam jet fragmentation processes modeled in HIJING using Lund/Fritiof strings. The initial energy density reached in such collisions can be estimated using the Bjorken formula

$$\epsilon(\tau_0) \approx \frac{1}{\pi R^2 \tau_0} \frac{dE_T}{dy} \quad (2.4)$$

For $p_0 \sim 1 - 2$ GeV, $dE_T/dy \sim 400 - 2000$ GeV, and so $\epsilon(\tau_0 \sim 0.5 \text{ fm}/c) > 10 \text{ GeV}/\text{fm}^3$

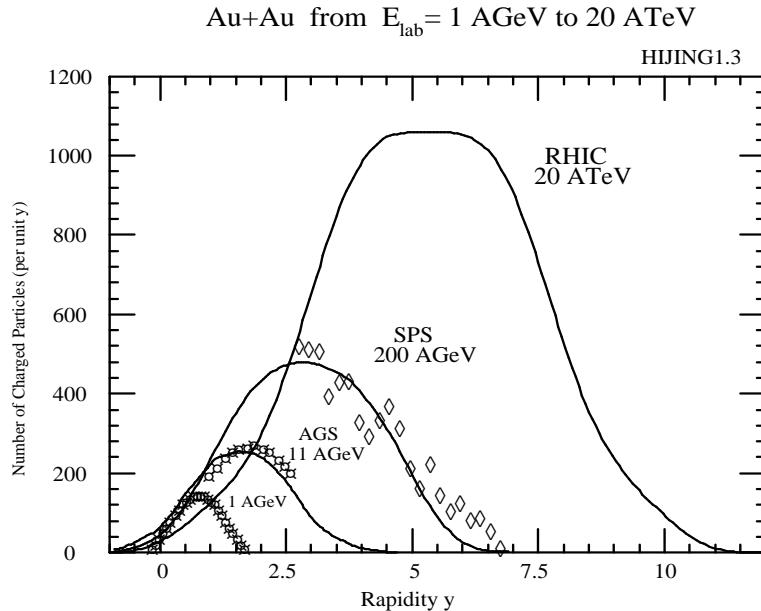


Fig. 5. Prediction of the height of "Mt. RHIC" at $E_{cm} = 100 \text{ AGeV}$ based on HIJING²¹⁾ event generator from Quark Matter 95²³⁾. Comparison to measured charged particle rapidity densities in $Au + Au$ reactions from $E_{lab} = 1, 10, 200 \text{ AGeV}$ is also shown.

should be easily reached, well inside the the deconfinement phase of QCD. At SPS energies, on the other hand, my estimates indicate that nuclear collisions may just reach the transition region and depart from that region in a very short time.

Since the the time of this talk, provocative and somewhat overstated press releases²⁴⁾ have been issued from CERN stating that "the experiments on CERN's Heavy Ion programme presented compelling evidence for the existence of a new state of matter in which quarks, instead of being bound up into more complex particles such as protons and neutrons, are liberated to roam freely. ... We now have evidence of a new state of matter where quarks and gluons are not confined."

As discussed below, I disagree with the above interpretation of that truly impressive body of data. What is compelling is that *some* form of matter, much denser than ever studied before, was created. Inferences about quark and gluon degrees of freedom are based on qualitative scenarios and schematic models. At the relatively low momentum scales accessible at SPS energies, the quarks and gluon degrees of freedom in the dense matter are mostly not resolvable. Even at the highest transverse momentum, the pion spectra were shown to be very sensitive to nonperturbative model assumptions such as to the magnitude of intrinsic momenta and soft initial state interactions²⁵⁾. The dynamics of the non-perturbative beam jet fragmentation and hadronic final state interactions cannot be disentangled at SPS²⁶⁾. It is useful to recall that in experiments on $p\bar{p}$ scattering, it was only possibly to see unambiguous

evidence for the tell-tale Rutherford scattering of point-like partons when collider energies $\sqrt{s} > 200 - 2000$ GeV became available. At RHIC high $p_{\perp} > 10$ GeV probes become kinematically available and hence very small wavelength resolution of partonic degrees of freedom finally becomes kinematically possible. While there is an abundance of interesting signatures showing that dense matter was formed at the SPS (through the non-linear in dependence of several observables on multiplicity or A), the bottom line is that those data have said nothing about whether the QCD predictions in Figs 1-3 are correct or not. We simply need higher resolution. RHIC, with its factor of ten increase in C.M. energy reaches a factor of ten deeper into the new phase reaches. Coupled with the availability of ten times shorter wavelength probes, it should finally become possible to actually see direct evidence of “freely roaming quarks and gluons”.

2.1. Global Signatures of Collective Dynamics

The simplest but often ignored global barometer of collectivity in nuclear reactions is the A and energy dependence of the transverse energy and charged particle rapidity density. At RHIC energies, HIJING predicts that initial transverse energy density in central $A + A$ collisions scales nonlinearly with A

$$\frac{dE_{\perp}}{dy} \approx 1 \text{ GeV } A^{1.3} \left(1 + \log \frac{\sqrt{s}}{200}\right) \quad (2.5)$$

This leads to about 1 TeV per unit rapidity. In¹⁷⁾, on the other hand, it was found that gluon saturation could limit the A dependence to approximately linear, $E_{\perp} \sim A^{1.04}$, but with a value several times that of HIJING. In Fig.(4), the initial gluon density actually grows less than linear $A^{0.92}$ in that model. The $A^{1.3}$ scaling of HIJING with its conservative $p_0 = 2$ GeV scale fixed by $p\bar{p}$ data is simply due to the number of binary interactions via (2.3). The initial energy density in HIJING varies approximately as

$$\epsilon_0 \approx 0.6 \text{ GeV/fm}^3 A^{0.63} \left(1 + \log \frac{\sqrt{s}}{200}\right) . \quad (2.6)$$

In¹⁷⁾ its magnitude and scaling are predicted to go as $\epsilon(\tau = 1/p_{sat}) \approx 0.1 A^{0.5} s^{0.38}$.

If local equilibrium is achieved and maintained, then a very basic prediction of hydrodynamics is that longitudinal boost invariant expansion together with $p dV$ work done by pushing matter down the beam pipe will cool the plasma and convert some its random transverse energy into collective longitudinal kinetic energy. For an equation of state, $p = c_s^2 \epsilon$, this cooling and expansion causes the energy density to decrease with proper time as

$$\epsilon(\tau) = \epsilon(\tau_0) \left(\frac{\tau_0}{\tau}\right)^{1+c_s^2} \quad (2.7)$$

Entropy conservation leads to a conservation of $\tau n(\tau)$, where n is the proper parton density. At least if the matter is initially deep in the plasma phase, then (as seen in Fig.3) longitudinal will be done with $c_s^2 \approx 1/3$. Consequently, the transverse energy per particle should decrease by a factor 2-3 before freeze-out as^{27), 17)}

$$e_{\perp}(\tau) = \frac{dE_{\perp}}{dN} = e_{\perp}(\tau_0) \left(\frac{\tau_0}{\tau} \right)^{c_s^2} \quad (2.8)$$

However, dissipative effects due to finite mean free paths reduce the effective pressure in any system. For the Bjorken expansion, the relaxation time, $\tau_c = 1/(\sigma_T n) \propto \tau$, then increases with time as n decreases. Numerical solution of 3+1 D transport equations with pQCD cross sections, $\sigma_T \sim 2$ mb, indicate that dissipation reduces the transverse energy loss for HIJING initial conditions rather significantly (see detailed comparisons in³⁷⁾). Ideal hydrodynamics predicts that about one half of the initial produced transverse energy goes into longitudinal work

It is important to keep in mind that the commonly assumed freeze-out prescription with τ_f fixed on a fixed freeze-out energy density hypersurface, $\epsilon(\tau_f) = \epsilon_f \approx 0.15$ GeV/fm³ is only a rough prescription that is never accurate³⁸⁾. As the interaction size decreases (A or multiplicity decreases), the effective speed of sound due to dissipation decreases and the system freezes out earlier. A detailed study of the A or multiplicity dependence of dE_{\perp}/dy and e_T is needed to calibrate the interplay of pdV work and dissipation on these barometers.

One of the major experimental discoveries of WA98, NA49 and the other SPS experiments is that at those energies dE_{\perp}/dy as well as dN/dy scale with A or wounded nucleon number nearly linearly²⁸⁾ as shown in Fig.(6). Both the E_{\perp} and the charge multiplicity increase as $\sim A^{1.07}$. These findings differ from the VENUS model, which has considerable nonlinearity due to the assumed sea string contributions. In fact, simple Glauber wounded nucleon models reproduce very well the nearly linear correlation between E_{\perp} and the veto calorimeter (spectator) energy observed in all experiments at SPS³⁰⁾. The implications of these data depend on the A dependence of the initial conditions of course. One view¹⁷⁾ is that the initial e_T can scale arbitrarily with A , but because perfect local equilibrium is maintained up to a critical sharp freeze-out hypersurface, the final E_T and e_T always scale linearly with A . My view is that at the SPS, pQCD is mostly inapplicable to bulk phenomena and the linear dependence arises from additive nature of soft beam fragmentation together with the *absence* of pdV work at early times. If the QGP transition region is just barely reached, as I believe without experimental proof, then the softness of the QCD equation of state with $c_s^2 \ll 1/3$ seen in Fig.(3) and dissipation can conspire to prevent the dense matter from performing longitudinal work. However, it is impossible to tell from the data whether the observed null effect is then due to a low pressure Hagedorn resonance gas of hadrons or to

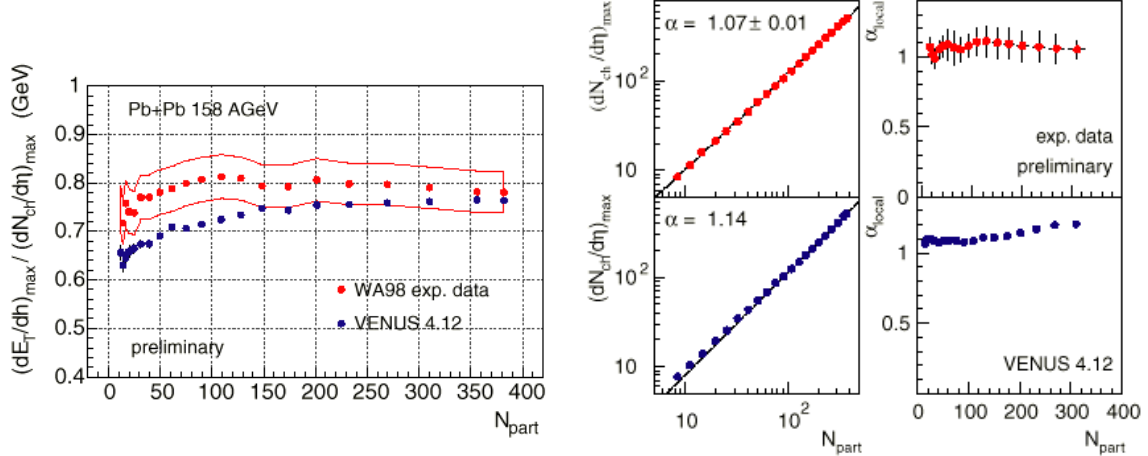


Fig. 6. Scaling of transverse energy per charged particle and and the charged particle rapidity density with number of participants in $Pb + Pb$ from H. Schlagheck et al WA98²⁸⁾. The nearly linear scaling in the number of participants can be interpreted as no longitudinal work was done by the lazy dense matter at the SPS.

a low pressure lazy “plasma” with $c_s \ll 1$. One has to go to higher energies to the plasma a chance to work.

In spite of the above remarks, ideal Euler hydrodynamic calculations have in fact been able to fit the null effect in the data quite well. This is possible by assuming arbitrary initial conditions chosen such that that after hydro does its work, the final results just happens to reproduce the data. An illustration of this degree of freedom is shown in Fig.(7) from³¹⁾. By adjusting the initial four velocity field appropriately, the calculated final pion distributions can be made to reproduce the data starting from two completely different initial energy density profiles. The same good fit to data can be obtained also for *ANY* assumed equation of state of dense matter simply by readjusting the initial conditions appropriately. Therefore, it is not surprising that even hand calculator fireball models are able to fit much of the data *without* invoking any dynamical or thermodynamical assumptions about the properties of dense matter prior to freeze-out^{33), 34)}. It is clear that inferring the existence of freely roaming quarks and gluons based on such fits is impossible^{35), 24)}.

In order to use the global barometers to search for evidence of collective phenomena in dense matter at RHIC, it is first necessary to eliminate the freedom to choose arbitrary initial conditions³²⁾. At collider energies, pQCD^{17), 18), 19), 20)} and non-Abelian field techniques^{16), 36)} provide the needed theoretical calibration tools to fix initial conditions At RHIC and LHC, the initial plasma is expected in any case to be so deep in the deconfined phase that the soft $p \ll \epsilon/3$ transition region and dissipation cannot spoil the longitudinal work as is the case at SPS. From detailed covariant transport calculations^{37), 38)} the barometric evidence

for longitudinal work should finally be observable in spite of finite mean free path effects. Deconvolution of the equation of state and dissipative corrections requires however a detailed study of the A and multiplicity dependence of the global E_T barometer.

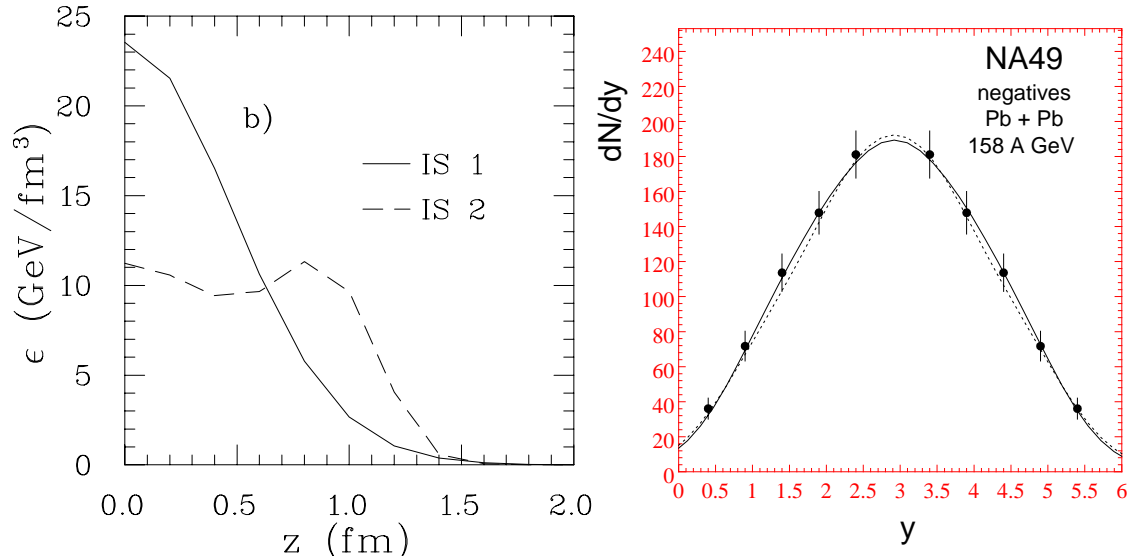


Fig. 7. Some different initial conditions that lead with suitable initial velocity fields via ideal hydrodynamics to same final observable pion rapidity density at SPS from ref. ³¹⁾.

This is the first important signatures to look forward to at RHIC. While it is not possible to converge on why no longitudinal work was observed at the SPS, a positive signature at RHIC would render such discussion mute. We can only be sure that a plasma was created if it does something collective! The global E_T and multiplicity systematics as a function of centrality as well as A therefore provide key handles in this search.

§3. Transverse Flow

In contrast to global transverse energy barometer a completely different measure of barometric collectivity is afforded by the study of the triple differential distributions, $dN/dyd^2\vec{p}_\perp$. Already at sub-luminal Bevalac energies (< 1 AGeV), azimuthally asymmetric collective directed and elliptic flow were discovered long ago. For non central collisions, $b \neq 0$, the asymmetric transverse coordinate profile of the reaction region leads to different gradients of the pressure as a function of the azimuthal angle relative to beam axis. This leads to a “bounce” off of projectile and target fragments in the reaction plane and to azimuthally asymmetric transverse momentum dependence of particles with short mean free at mid rapidities. This phenomenon has now been observed at both AGS and SPS energies as well. It will certainly be there also at RHIC and LHC. In Fig.(8) the first two Fourier components

of the azimuthal flow patterns are shown:

$$\frac{dN}{dyd^2p_{\perp}} = v_0(1 + 2v_1 \cos(\phi - \phi_R) + 2v_2 \cos(2(\phi - \phi_R)) + \dots) \quad (3.1)$$

Azimuthal asymmetric collectivity is clearly observed at the SPS. The important question

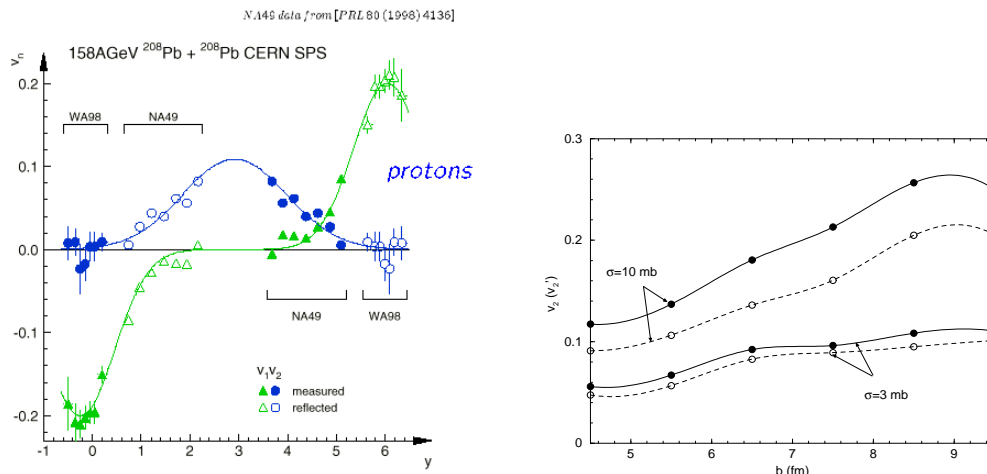


Fig. 8. (left) Azimuthal flow analysis in $Pb + Pb$ from H. Schlagheck et al WA98^{28), 39)} and NA49 data²⁹⁾. (Right) Predicted dependence of v_2 at mid rapidity $Au + Au$ at RHIC from parton cascade calculations ZPC⁴²⁾ with HIJING initial conditions.

is how this type of barometer could serve to help search for evidence of the QCD transition. Unlike the global E_{\perp} barometer discussed in the previous section, transverse flow can develop at later times because the gradients are controlled by the transverse size of the nucleus, not the proper time interval relative to formation. In⁴⁰⁾ the idea was proposed that one could use v_2 for example to study the predicted softening of the QCD equation of state. Typically, hydrodynamics calculations lead to a factor of two smaller v_2 for an equation of state with a soft critical point as in Fig 3 versus one in which the speed of sound remains $1/\sqrt{3}$. Searches for anomalous v_2 dependence as well as v_1 are underway⁴¹⁾. As with the global barometer, dissipation can of course also simulate a soft equation of state. In ref⁴²⁾ we studied the dependence of v_2 on the transport parton cross section. The results shown in Fig(8) for HIJING initial conditions indicate that there is indeed a significant reduction of v_2 relative to hydrodynamics, but that the impact parameter (multiplicity) dependence of that observable can again be used to disentangle the equation of state versus viscosity effects as in the case of the global E_T barometer.

§4. The QGP Stall and Time delay

Hadron interferometry has been developed into a fine art in heavy ion collisions to image the space-time region of the decoupling 4-volume. In⁴⁵⁾ it was proposed that a possible signature of the QGP phase transition would be a time delay associated with very slow hadronization. The plasma "burns" into hadronic ashes along deflagration front that moves very slowly if the entropy drop across the transition is large⁴⁶⁾. Fig.9 shows the evolution of a Bjorken cylinder with time and transverse coordinate from a hydrodynamic simulation with different equations of state from⁴⁴⁾. The main point to note is that time delay is a robust

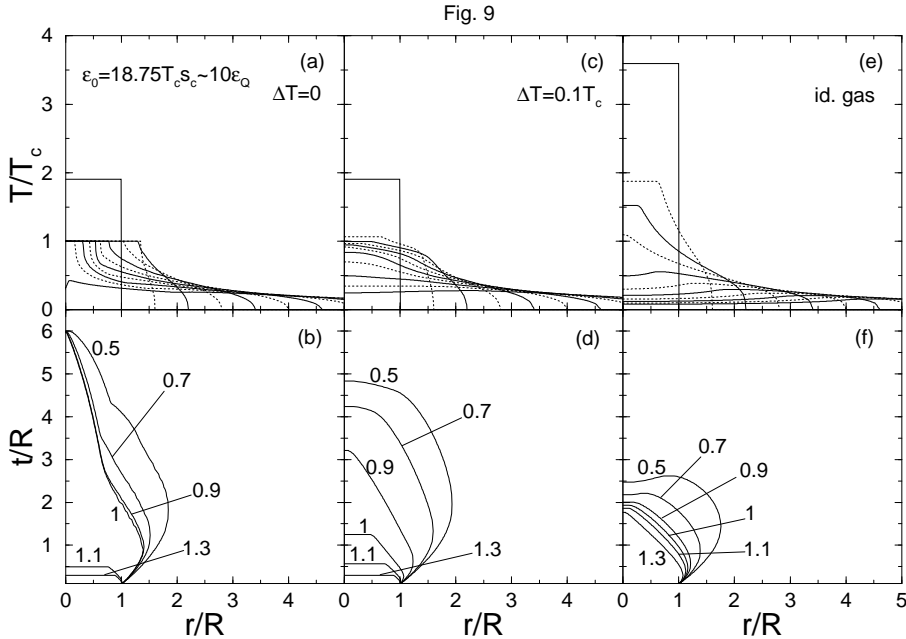


Fig. 9. Evolution of isothermal contours for a boost invariant QGP cylinder with initial energy density ~ 20 GeV/fm³ for different equations of state from ref.⁴⁴⁾. For a strong first order transition the QGP "stall" is very strong, but it also remains significant even if the transition is only a rapid cross over consistent with Fig.3. For an ideal gas with $p = \epsilon/3$ on the other hand, the freeze-out time scale and radius are approximately equal. An experimental probe of this decoupling geometry is provided by pion or kaon interferometry.

generic signature of a rapid cross over transition of the entropy density. In particular the "stall" is expected even for a smooth cross-over transition as long as the width $\Delta T/T_c < 0.1$. However, its magnitude also depends on the entropy drop across that region. The figures are for an entropy drop by a factor 10 consistent with the lattice QCD results. Unfortunately, as noted before lattice QCD has not yet resolved the hadronic world below T_c due to numerical problems. If the entropy jump is much smaller, then this signature would also disappear.

High statistics measurements of pion and kaon interferometry searches for time delay at AGS and SPS have come up empty handed thus far. No time delay has ever been observed in

any nuclear reactions thus far. This could be due to (a) the absence of a large rapid entropy drop in real QCD, or (b) to unfavorable kinematic conditions at AGS and SPS energies. From the hydrodynamic calculations in ⁴⁴⁾, it was found that a large time delay signal requires that the initial energy density be deep within the plasma phase. The slow deflagration waves seen in Fig.9 do not arise if the initial energy density is close to the transition region because the initial longitudinal expansion cools the plasma too rapidly. The optimal conditions to see this effect was predicted ⁴⁴⁾ to occur at RHIC energies. For much higher energies (LHC), on the other hand, the transverse expansion of the plasma has too much time to develop and that spoils the possibility of a slowly burning plasma stall. I note that further work ⁴⁷⁾ has shown that high p_{\perp} kaon interferometry adds an especially sensitivity handle in the search for this time delay signature. If ever observed, the time delay signature would be smoking gun that a new form of matter with bulk collective properties was created.

§5. The J/ψ puzzle

In 1986, Matsui and Satz proposed an intriguing direct measure of the transmutation of the $q\bar{q}$ forces in Fig. 1. The idea was that J/ψ can form in the vacuum because the confining Luscher potential can bind a $c\bar{c}$ pair into that vector meson. If that pair were placed in a hot medium in which the chromo-Debye screening potential is short ranged, then above the temperature where the screening length is smaller than the J/ψ radius, the $c\bar{c}$ would become unbound and the charm quarks would emerge from the reaction region as an open charm $D\bar{D}$ pair. They thus predicted that J/ψ suppression would be a smoking gun for the deconfinement transition.

J/ψ suppression was first seen in 1987 in $O + U$ reactions by NA38. Since then this smoking gun has (unfortunately) never stopped smoking! J/ψ suppression seems to be as ubiquitous as the Yukawa potential. It is now clearly observed in $p + A$ reactions as seen in Fig.(10). High mass Drell-Yan pairs, on the other hand, formed via $q\bar{q} \rightarrow \ell\bar{\ell}$ was observed to scale perfectly linearly with the number of binary collisions. This is because lepton pairs suffer no final state interactions and the quark initial state (Cronin) interactions are invisible in p_{\perp} integrated DY yields.

J/ψ are suppressed on the other hand as $(AB)^{0.9}$ due to some nuclear effect that is independent of QGP production. In the recent Pb+Pb analysis an excess 25% suppression of J/ψ was observed. NA50 claims that this enhanced suppression relative to the $(AB)^{0.9}$ trend from lighter projectile $p, O, S + U$ data is finally the real smoking gun ⁴⁸⁾. From the suppression pattern in Pb as observed as a function of centrality (see Fig.(11)), NA50 has now claimed that in fact “Together with the results previously established by the NA38 and

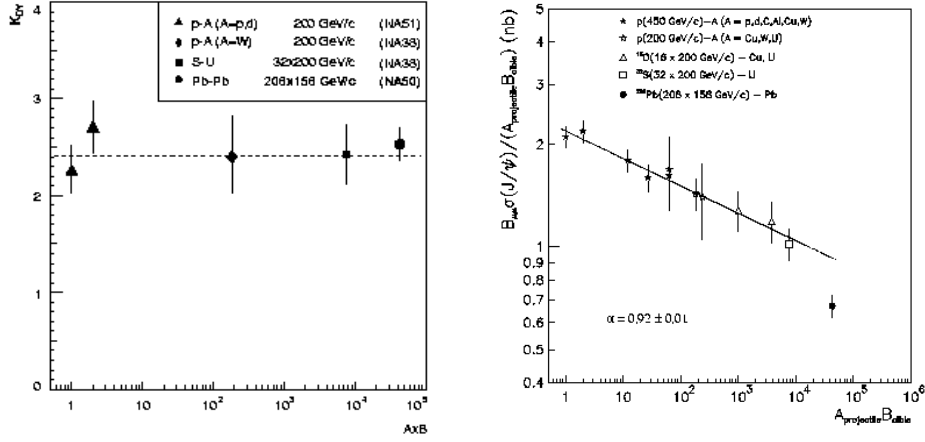


Fig. 10. Drell-Yan scales as $(AB)^1$ very accurately from NA38, NA50. However, J/ψ scale as $(AB)^{0.9}$ showing that their production is suppressed with increasing nuclear volume even in $p + A$ reactions Ref. 48). The "anomalous" suppression in $Pb + Pb$ is the 25% deviation from the empirical $(AB)^{0.9}$ expectation.

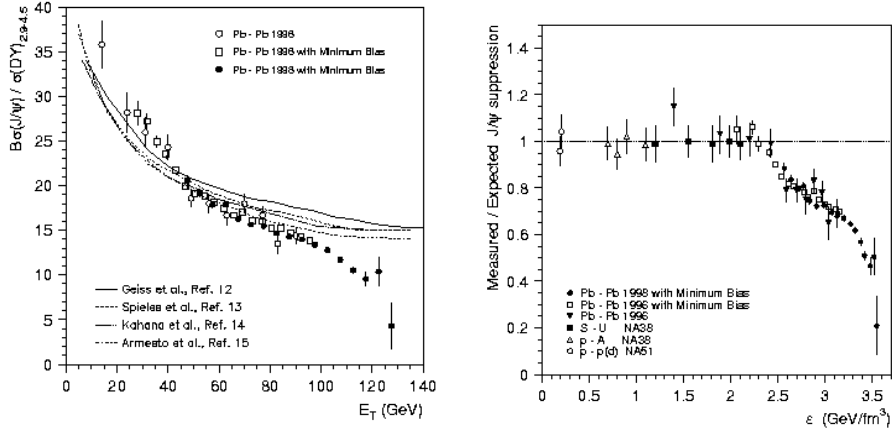


Fig. 11. "Evidence for deconfinement of quarks and gluons from the J/ψ suppression pattern measured in Pb Pb collisions at the CERN-SPS" claimed by NA50 in Ref. 48). The curves on left show transport theory estimates for hadronic final state dissociation. The enhanced suppression relative to $\exp(-\sigma_N \rho_0 L)$ nuclear suppression observed in $p + A$ and $S + U$ is shown versus a rough estimate of the initial energy density (this scale is uncertain to at least a factor of two for each point!).

NA50 collaborations, a rather clear picture emerges, indicating a step-wise pattern, with no visible saturation in the collisions generating the highest energy densities and temperatures. Our observations exclude the presently available models of J/ψ suppression based on the absorption of the J/ψ mesons by interactions with the surrounding hadronic (confined) matter. The first anomalous step can be understood as due to the disappearance of the χ mesons, responsible for a fraction of the observed J/ψ yield through its (experimentally

unidentified) radiative decay. In proton induced collisions this fraction is around 30-40%. The second drop signals the presence of energy densities high enough to also dissolve the more tightly bound J/ψ charmonium state.”

While the deviation from the empirical $(AB)^{0.9}$ scaling is very clear, the dynamic origin of the effect is far from clear in my opinion. As shown by the several curves in Fig.(11), a $\sim 50\%$ drop in the J/ψ yield as a function of E_T is consistent with final state co-moving hadronic absorption. While the details are not reproduced accurately, large theoretical uncertainties about several key dynamical ingredients preclude precise comparisons at this time. It is important to emphasize that the so called “conventional hadronic” models suffer from just as large theoretical uncertainties as the plasma scenario models. Key uncertain elements include (1) the dynamical treatment of cold nuclear absorption responsible for the $AB^{0.9}$ suppression even in $p + A$, (2) the unknown hadronic $M + \psi \rightarrow D\bar{D}X$ reaction rates, and (3) the actual density evolution, $\epsilon(\vec{x}, t)$ needed in order to make more precise calculations. Only a schematic “octet model” of pre-hadronization $c\bar{c}$ interactions in cold nuclei has been used in the above transport models to address the first effect. That this is highly uncertain is shown in the work of Ref.⁵¹⁾. The observed J/ψ production cross section even without final state interactions is suppressed as follows:

$$\sigma_{AB \rightarrow \psi X} = \int d\sigma_{AB \rightarrow c\bar{c}} F_{c\bar{c} \rightarrow \psi}(q^2) \quad (5.1)$$

where F is the formation probability of the ψ from a $c\bar{c}$ that emerges from the cold nuclear target with an invariant mass $q^2 < 4M_D^2$. If the pre-resonance $c\bar{c}$ pair multiply scatters in the nucleus random walk would increase $q^2 \rightarrow q^2 + \delta q^2(\sigma\rho L)$ linearly with nuclear thickness as shown by the curve G in Fig.(12). This leads to an approximate exponential suppression that can be fit well by an approximate Glauber nuclear absorption factor ansatz, $\exp(-\sigma_{eff}\rho L)$ if a Gaussian assumption is made. This Gaussian model can thus account for the observed $(AB)^{0.9}$ scaling light projectiles. *However*, it was shown in⁵¹⁾ that if the power law tails due to induced radiation in the medium is included (resulting from the multiple Rutherford rescattering of the color octet $c\bar{c}$), then an additional nonlinear suppression in the nuclear thickness L *could* result (curve P). This is because radiation provides another way to increase the invariant mass of the pre-resonance $c\bar{c}$ that can further reduce the probability for the pair to fit inside the ψ wavefunction. While this model is also schematic, I feel that it captures an important element of pre-formation transient dynamical effects in nuclei that can serve as additional sources of nonlinear suppression, without even considering the sought after suppression in the comoving dense matter. The transport model curves in Fig.11 co-moving dissociation possesses and pre-resonance nuclear dynamics as in Fig.12 should be combined in future analysis searching for the dynamical origin of beyond nuclear Glauber absorption

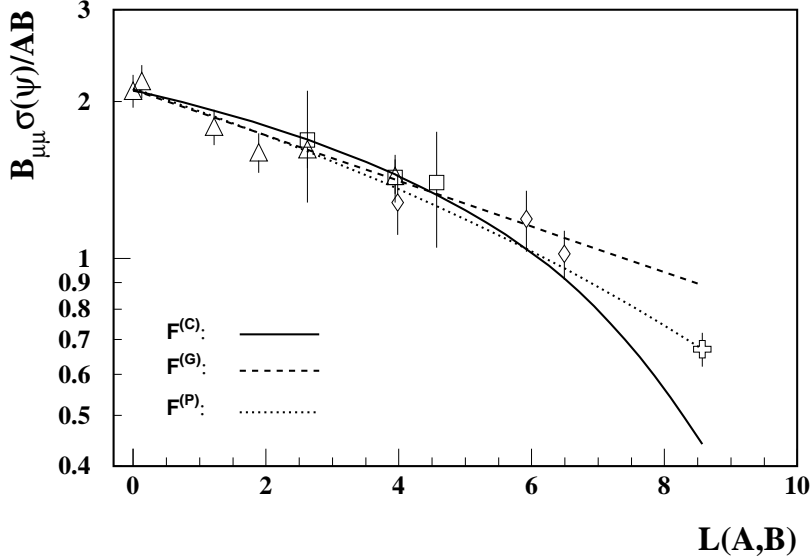


Fig. 12. Sensitivity of “pre-resonance” J/ψ nuclear absorption to details of color octet models of $c\bar{c}$ interactions in a nuclear medium from Qiu et al⁵¹⁾. The curve marked P for power law accounts for the anomalous absorption seen in $Pb+Pb$ and deviated from Gaussian Glauber-like G expectations.

in $Pb + Pb$.

Therefore, the claim of anomalous suppression cannot rest therefore merely on generic enhanced suppression in Pb . It must and has been made on the possible existence of singular “step-like” structure of the suppression pattern. The evidence for ”steps” is however the weakest link experimentally because a rigorous χ^2 test including the substantial systematic errors in the E_T scale has yet to be performed. This very difficult experiment has fought valiantly for years to reduce the systematic errors associated with calibration of E_T , thick target multiple interactions, and calibrating the Drell-Yan and other backgrounds. This is illustrated in Fig.(13) where plasma scenario fits⁵²⁾ to 1997 data are also shown. In Fig.(14) recent plasma scenario fits⁵³⁾ to the latest data show how much the data has evolved (see⁴⁸⁾ for details). It is also clear from Figs.(13,14) that the plasma scenario step-function models while capable of fitting the data cannot be considered as prediction of QCD. Percolation models serve to motivate the steps.

Nevertheless, if the “step-like” suppression pattern survives further experimental scrutiny, it would certainly be the most dramatic nonlinearity observed at SPS. In this connection, it is also important to remark that the energy density scale in Fig.(11 b) is uncertain to at least a factor of two. There is no direct experimental measurement of the initial energy density. The energy scale there is inferred from a RQMD model calculation. However, as shown in Fig.(7) a nice hydro fit to the data could be obtained with an initial energy density

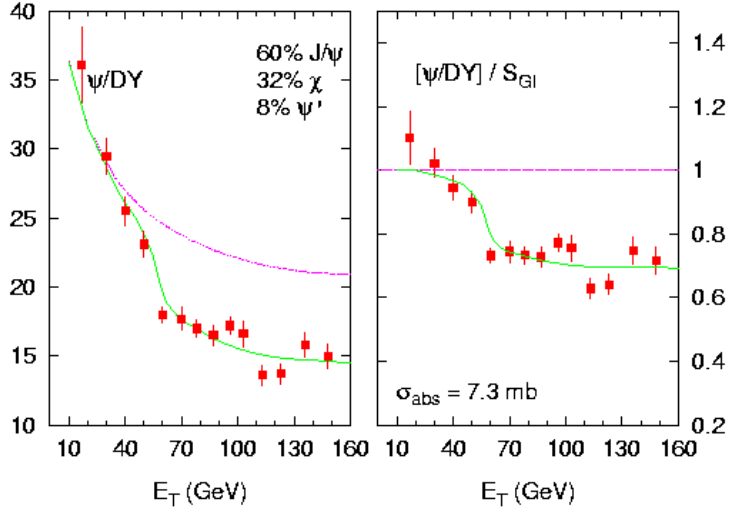


Fig. 13. Plasma scenario step function fits from Kharzeev et al⁵²⁾. to NA50 step-like J/ψ suppression in $Pb + Pb$ at Quark Matter 97. Left is the ψ/DY ratio as a function of the E_T scale at that time. Right is the ratio normalized to the empirical nuclear suppression effect.

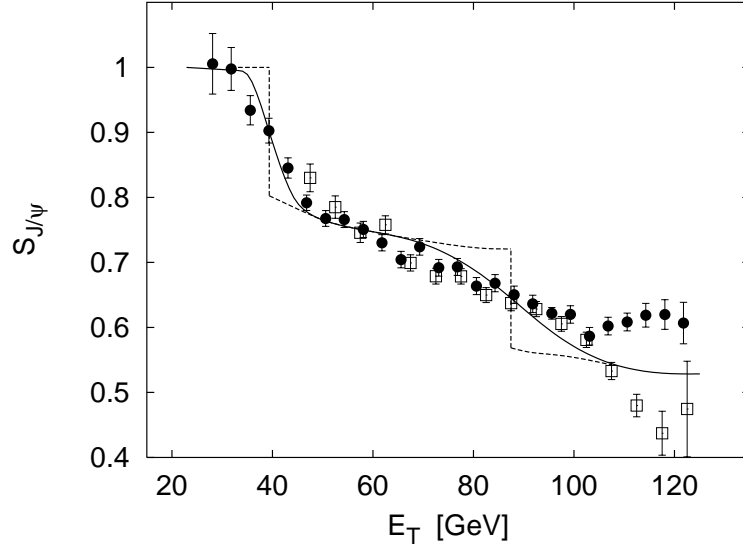


Fig. 14. Percolation model step-function fits to the ψ survival probability normalized to the empirical nuclear suppression effect from H. Satz, Quark matter 99⁵³⁾. Open square NA50 data are from thinner target runs with $Pb + Pb$.

ten times higher than assumed in Fig.11 b.

Given the boldness of the NA50 claims, it is important to scrutinize both the experimental and theoretical foundations on which those claims are made. In science guilt is to assumed until innocence is proven. Based on the previous discussion, I remain skeptical.

An additional problem with the plasma scenario interpretations can be seen from the

observed E_T dependence of the J/ψ p_\perp spectra in Fig.(??). Standard Glauber multiple collisions lead to a random walk in transverse momentum that are expected to lead to⁵⁴⁾

$$\langle p_\perp^2 \rangle_{AB} = \langle p_\perp^2 \rangle_{pp} + \frac{L}{\lambda} \delta p_\perp^2 \quad (5.2)$$

this is found to hold⁴⁹⁾ in all reaction including $Pb + Pb$. In contrast, in the plasma scenario⁵⁵⁾, only those ψ are expected to survive that are near the surface where the nuclear depth L is small. Thus the prediction as shown in Fig(??) was that the $\langle p_\perp^2 \rangle$ should begin to DECREASE with increasing E_T . This was not observed^{49), 50)}. Clearly, much more work

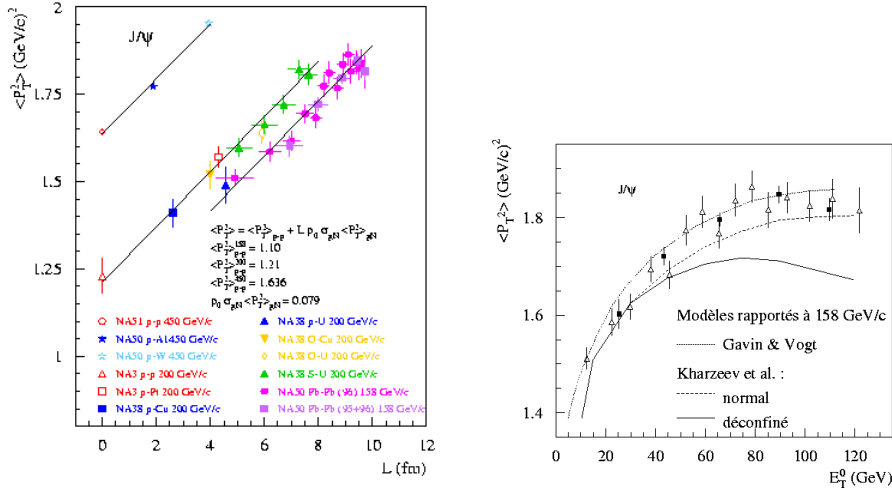


Fig. 15. The mean transverse momentum of the J/ψ ⁴⁹⁾ shows clear evidence of multiple scattering in the nuclear target as expected⁵⁴⁾ from Glauber theory. Even in $Pb + Pb$ the increase of the p_T is understood from the same mechanism in contradiction⁵⁰⁾ to predictions based on the plasma scenario, where at high E_T , the surviving ψ are expected to have been produced only near the nuclear surface regions⁵⁵⁾.

is required to sort out the very interesting suppression pattern observed by NA38,NA50. Experimentally, the claims would carry considerable more punch if similar "step-wise" patterns were observed in other systems, e.g. $Xe + Xe$ suitably shifted in E_T due to the expected smaller energy densities achieved. While it is not likely that such further measurements will get done, they will be at RHIC. A clear prediction by H. Satz at QM99⁴³⁾, was that under RHIC conditions of higher energy density, the same step wise pattern as in Fig.(14) should be observable in $Cu + Cu$ interactions. PHENIX will provide a definitive test of this prediction soon.

§6. The High p_{\perp} Frontier

One of the new areas that RHIC will open in the experimental search for the next Yukawa phase of QCD is high transverse momentum (short wavelength) jet probes. The rates of jet production and its fragmentation in the vacuum are well understood. The new physics here is the study of partonic interactions at extreme densities through the phenomenon of jet quenching⁵⁶⁾. Final state interactions of a jet in a dense QGP are expected to induce a large radiative energy loss⁵⁷⁾. In fact, it was discovered in by BDMPS⁵⁸⁾ that non-Abelian energy loss is in fact non-linear as a function of the thickness of the medium. Tests of this and other aspects of non-Abelian multiple collision dynamical will be possible at RHIC⁵⁹⁾.

At SPS energies, this physics is out of reach given the dominance of nonperturbative effects as shown in Fig.(16) from ref.²⁵⁾. HIJING accidentally fits the WA98 data with or without jet quenching. At the SPS no clean separation of soft and hard dynamics is kinematically possible. However, at RHIC energies, the power law tails of the single inclusive distributions stick far enough above the confusing soft "noise" to gain sensitivity to the form of the non-Abelian dE/dx as seen in Fig.(16). This problem is closely related also

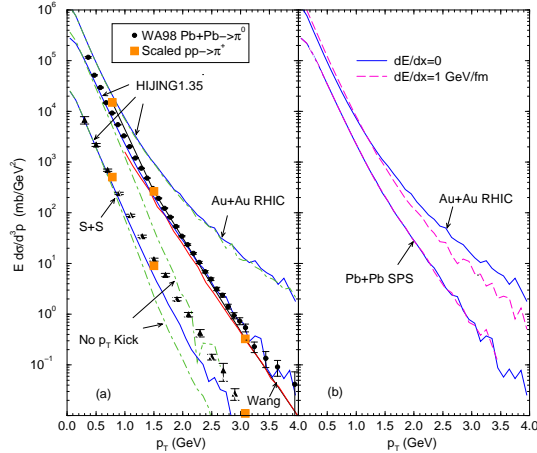


Fig. 16. Jet quenching at SPS vs RHIC from ref.²⁵⁾ compared to WA98 data. At RHIC the power law tail extends finally far enough above the nonperturbative "noise" to make jet quenching observable.

to the problem of pre-resonance J/ψ absorption discussed previously⁵¹⁾. Understanding jet quenching is also prerequisite in testing the dynamical assumptions of recent covariant parton transport theories^{38), 37)}.

§7. Summary

The next Yukawa phase is awaiting discovery. The SPS data have provided many intriguing indirect hints that new physics is operating in dense matter. Many puzzles, claims and counter claims remain because at SPS energies, both hadronic and partonic models have partial overlapping domains of validity. This “duality” is analogous to the problem of interpreting the R factor in e^+e^- collisions below $\sqrt{s} < 10$ GeV. The ratio of hadronic to leptonic production cross sections only reaches the magic 11/3 of pQCD above that threshold region where the $s\bar{s}$, $c\bar{c}$, $b\bar{b}$ vector mesons dominate the nonperturbative hadronic physics. Similarly SPS is at the door-step where hadronic resonances begin to melt away and a pQCD continuum description start to become more relevant.

With RHIC the factor of ten increase in the initial energy density will be unambiguously in the QGP continuum. The matter so formed will also have much more time to develop collective signatures. The factor of ten smaller wavelength probes will finally allow experimentalists to resolve (i.e. see) the quark and gluon degrees of freedom of that plasma. Direct observation of longitudinal work, transverse azimuthal collectivity, time delay, step-wise J/ψ suppression in $Cu + Cu$, and jet quenching will offer direct signatures of the sought after new phase of QCD matter.

Acknowledgements

I thank Profs. H. Horiuchi and T. Hatsuda for organizing this Yukawa symposium. I would especially acknowledge Mayor Baba and the city of Nishinomia their support of this symposium series. This work was supported by the Director, Office of Energy Research, Division of Nuclear Physics of the Office of High Energy and Nuclear Physics of the U.S. Department of Energy under Contract No. DE-FG-02-93ER-40764.

References

- [1] H. Yukawa, Proc. Phys.-Math. Soc. Jpn. Ser.3, **17** (1935) 48.
- [2] O. Klein, Z. Phys. **37** (1926) 895.
W.
- [3] W. Pauli, *Meson Theory of Nuclear Forces*, (Interscience Pub. Inc., New York 1946).
- [4] R. Machleidt, *The Meson Theory of Nuclear Forces and Nuclear Structure*, in *Advances in Nuclear Physics*, **19**, eds. J.W. Negele and E. Vogt,(Plenum Press, New York, 1989), chap.2.
- [5] P. Debye and E. Hückel, Z. Phys. **24** (1923) 185.

- [6] M. Lüscher, K. Symanzig, and P. Weise, NPB 173 (1980) 365.
- [7] J. B. Kogut, Rev. Mod. Phys. 55 (1983) 775.
- [8] J. Garden [UKQCD Collaboration], hep-lat/9909066.
- [9] M. Gao, Phys. Rev. D40 (1989) 2708.
- [10] O. Kaczmarek, F. Karsch, E. Laermann and M. Lutgemeier, hep-lat/9908010.
- [11] M. Gao, Phys. Rev. **D41**, 626 (1990).
- [12] A. K. Rebhan, Nucl. Phys. **B430**, 319 (1994)
- [13] C. Bernard *et al.* [MILC Collaboration], Phys. Rev. **D55**, 6861 (1997) [hep-lat/9612025].
- [14] N. Christ, R. Mawhinney, et al, QCDSF project, <http://phys.columbia.edu/~cqft/>, RBRC supercomputer center: http://www.ccd.bnl.gov/riken_bnl/riken.html
- [15] CP-PACS project: <http://www.rccp.tsukuba.ac.jp/>
- [16] L. McLerran and R. Venugopalan, Phys. Rev. **D49**, 2233 (1994) [hep-ph/9309289].
- [17] K. J. Eskola, K. Kajantie, P. V. Ruuskanen and K. Tuominen, Nucl. Phys. **B570**, 379 (2000) [hep-ph/9909456].
- [18] K. J. Eskola, K. Kajantie and J. Lindford, Nucl. Phys. **B323**, 37 (1989).
- [19] J. P. Blaizot and A. H. Mueller, Nucl. Phys. **B289**, 847 (1987).
- [20] M. Gyulassy and L. McLerran, Phys. Rev. **C56**, 2219 (1997) [nucl-th/9704034].
- [21] X. Wang and M. Gyulassy, Phys. Rev. **D44**, 3501 (1991).
- [22] X. Wang, Phys. Rept. **280**, 287 (1997) [hep-ph/9605214].
- [23] M. Gyulassy, Nucl. Phys. **A590**, 431C (1995) [nucl-th/9503024].
- [24] CERN Press Release 2/8/00: <http://press.web.cern.ch/Press/Releases00/PR01.00EQuarkGluonMatter.html>,
<http://cern.web.cern.ch/CERN/Announcements/2000/NewStateMatter/>,
http://webcast.cern.ch/Archive/Seminars/Special/New_state_of_Matter_10022000/
- [25] M. Gyulassy and P. Levai, Phys. Lett. **B442**, 1 (1998) [hep-ph/9807247].
- [26] S. A. Bass, M. Gyulassy, H. Stoecker and W. Greiner, J. Phys. G **G25**, R1 (1999) [hep-ph/9810281].
- [27] G. C. Nayak, A. Dumitru, L. McLerran and W. Greiner, hep-ph/0001202.
- [28] H. Schlagheck [WA98 Collaboration], Nucl. Phys. **A663&664**, 725 (2000) [nucl-ex/9909005].
- [29] S. A. Voloshin and A. M. Poskanzer, Phys. Lett. **B474**, 27 (2000)
- [30] D. Kharzeev, C. Lourenco, M. Nardi and H. Satz, Z. Phys. **C74**, 307 (1997) [hep-ph/9612217].
- [31] P. Huovinen, P. V. Ruuskanen and J. Sollfrank, Nucl. Phys. **A650**, 227 (1999) [nucl-th/9807076].

- [32] A. Dumitru and D. H. Rischke, Phys. Rev. **C59**, 354 (1999) [nucl-th/9806003].
- [33] U. Heinz, Nucl. Phys. **A661**, 140 (1999) [nucl-th/9907060].
- [34] A. Ster, T. Csorgo and B. Lorstad, Nucl. Phys. **A661**, 419 (1999) [hep-ph/9907338].
- [35] U. Heinz and M. Jacob, nucl-th/0002042.
- [36] A. Krasnitz and R. Venugopalan, hep-ph/9909203.
- [37] M. Gyulassy, Y. Pang and B. Zhang, Prog. Theor. Phys. Suppl. **129** (1997) 21; Nucl. Phys. **A626**, 999 (1997) [nucl-th/9709025].
- [38] D. Molnar, M. Gyulassy, New Solutions to Covariant Transport Theory, Columbia preprint CU-TP-973 (2000).
- [39] M. Aggarwal et al WA98, Nucl. Phys. A610 (1996) 200c.
- [40] J.-Y. Ollitrault, Phys. Rev. D **46** (1992) 229.
- [41] J.-Y. Ollitrault, Nucl. Phys. **A590** (1995) 561c; W. Reisdorf and H.G. Ritter, Annu. Rev. Nucl. Part. Sci. **47** (1997) 663.
- [42] B. Zhang, M. Gyulassy and C. M. Ko, Phys. Lett. **B455**, 45 (1999) [nucl-th/9902016].
- [43] S. A. Bass *et al.*, Nucl. Phys. **A661**, 205 (1999) [nucl-th/9907090].
- [44] D. H. Rischke and M. Gyulassy, Nucl. Phys. **A608**, 479 (1996) [nucl-th/9606039].
- [45] S. Pratt, Phys. Rev. C 49 (1994) 2722, Phys. Rev. D 33 (1986) 1314.
- [46] L. Van Hove, Z. Phys. C 21 (1983) 93,
M. Gyulassy, K. Kajantie, H. Kurki-Suonio, L. McLerran, Nucl. Phys. B 237 (1984) 477.
- [47] S. Bernard, D. H. Rischke, J. A. Maruhn and W. Greiner, Nucl. Phys. **A625**, 473 (1997) [nucl-th/9703017].
- [48] M. C. Abreu *et al.* [NA50 Collaboration], Phys. Lett. **B477**, 28 (2000).
- [49] O. Drapier, Thesis, Universit Lyon-I, 1998
- [50] J. L. Nagle and M. J. Bennett, Phys. Lett. **B465**, 21 (1999) [nucl-th/9907004].
- [51] J. Qiu, J. P. Vary and X. Zhang, hep-ph/9809442.
- [52] D. Kharzeev, Nucl. Phys. **A638**, 279C (1998) [nucl-th/9802037].
- [53] H. Satz, Nucl. Phys. **A661**, 104 (1999) [hep-ph/9908339].
- [54] S. Gavin and M. Gyulassy, Phys. Lett. **B214**, 241 (1988).
- [55] D. Kharzeev, M. Nardi and H. Satz, Phys. Lett. **B405**, 14 (1997) [hep-ph/9702273].
- [56] M. Gyulassy, M. Plümer, M.H. Thoma and X.-N. Wang, Nucl. Phys. A **538** (1992) 37c.
X.-N. Wang and M. Gyulassy, Phys. Rev. Lett. **68** (1992) 1480.
- [57] M. Gyulassy and X.-N. Wang, Nucl. Phys. B **420** (1994) 583.
- [58] R. Baier, Yu.L. Dokshitzer, A.H. Mueller and D. Schiff, Nucl. Phys. B **531** (1998)

403 and refs therein.

[59] M. Gyulassy, P. Lévai, I. Vitev, Nucl. Phys. B **571** (2000) 197.